Article

Ultrabright Red to NIR Emitting Fluorescent Organic Nanoparticles Made from Quadrupolar Dyes with Giant Two-Photon Absorption (2PA) in the NIR Region. Confinement Effect on Fluorescence and 2PA and Tuning of Surface Properties

Published as part of The Journal of Physical Chemistry virtual special issue "125 Years of The Journal of Physical Chemistry".

Paolo Pagano,[‡] Morgane Rosendale,[‡] Jonathan Daniel, Jean-Baptiste Verlhac, and Mireille Blanchard-Desce*

ACCESS | Metrics & More | Article Recommendations | SI Supporting Information

ABSTRACT: Fluorescent Organic Nanoparticles (FONs) are light-emitting, molecular-based nanoparticles that can be obtained from the nanoprecipitation of dedicated hydrophobic organic dyes in water. They represent a versatile family of water-soluble fluorescent nanotools whose luminescent properties can be tuned by bottom-up molecular engineering of their composing dyes. We recently reported on a quadrupolar red-emitting dye that yields spontaneously stealthy bare FONs which do not require coating to hinder interactions with cell membranes. Its quadrupolar design also hints to the possibility that it may be a strong two-photon absorber for bioimaging purposes. In this paper, we further investigate the two-photon absorption (2PA) of this dye and resulting FONs and report on a structure-related series of extended dyes engineered to yield NIR-emitting FONs. All dyes lead to stable, small (12−20 nm in diameter), and bright FONs. The experimental study reveals that molecular confinement strongly influences the fluorescence and 2PA properties of these dyes depending on the nature of the π-extended system. As expected, extension of the π-conjugated system induces a red-shift of the absorption and emission bands as well as an increase and spectral broadening of the 2PA responses in solution. Upon aggregation of the dyes within nanoparticles, a reduction of the fluorescence quantum yield is observed whose amplitude depends strongly on the nature of the π-conjugated systems. Interestingly, the peak 2PA cross sections increase upon confinement of the shortest dye, while a spectral broadening and slight red shift of the 2PA bands of the most extended dyes is observed. Taken together, these properties allow the most extended dye to yield very bright NIR-emitting FONs ($\varepsilon^{max}\Phi = 7 \times 10^6$ M^{-1} cm^{-1}, $\sigma_2^{max}\Phi = 4 \times 10^5$ GM). Interestingly, the nature of the π-conjugated system was also found to modulate the stealthiness of the resulting nanoparticles toward biological membranes. As a result, by fine-tuning the molecular design of the quadrupolar FON-composing dyes, we achieved NIR-absorbing, NIR-emitting, spontaneously stealthy small nanoparticles having record one- and two-photon brightness. Finally, we demonstrate that these FONs can be noncovalently surface-coated with a polycationic polymer, thanks to their highly negative surface potentials. This induces a reversal of their surface potential which in turn triggers their internalization within cells.
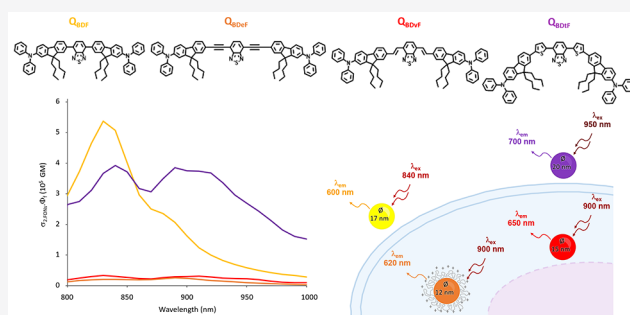
INTRODUCTION

Fluorescence microscopy is a powerful technique for imaging biological samples. Even though the majority of dedicated fluorophores absorb and emit in the UV−visible spectral region, the use of red to near-infrared (R-NIR) light is particularly favorable for in depth imaging. The first optical transparency window has indeed been identified around 650− 900 nm where the emission of endogenous fluorophores responsible for background noise[1] and the absorption and scattering by blood and fatty contents[2] are both at their lowest.

Two-photon (2P) microscopy[3] is currently one of the most favored methods to achieve NIR excitation. First, because the 2P process allows excitation of fluorophores at about twice the
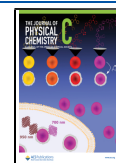
wavelength necessary for one-photon (1P) excitation (except in the case of symmetry-forbidden transitions), which usually means exciting at wavelengths higher than 700−800 nm. Second, because it displays an intrinsic sectional ability thanks to its nonlinear nature. As 2P excitation only occurs at the focal spot of the objective, only the fluorophores localized in the focal plane become visible. 2P microscopy thus greatly improves axial resolution while reducing photobleaching of the probes and photodamage of the samples. The capacity of a fluorophore to be excited by the 2P process is described by its two-photon absorption (2PA) cross-section σ_2, and its most critical parameter is its brightness $\sigma_2\Phi_f$, both expressed in Goeppert-Mayer (GM). Commercially available water-soluble organic fluorescent dyes exhibit low to modest 2P brightness values, rarely exceeding a few hundred GM and exceptionally reaching in the thousands.[4] The design and synthesis of 2P sensitive fluorescent organic probes displaying much larger cross sections has been a very fertile research field over the last two decades.[5−8] As far as bioimaging is concerned, R-NIR-emitting dyes are also of major interest as they benefit from easier detection deep in tissues.[9−11] Among various systems, molecular-based Fluorescent Organic Nanoparticles (FONs)[12,13] may prove to be good candidates to this aim. On the one hand, their organic nature allows for the fine-tuning of specific properties by molecular engineering, including morphological,[14,15] photophysical,[16,17] colloidal,[18] and surface[19,20] properties. On the other hand, nanoparticles (NPs) have had valuable developments in numerous biomedical fields that can benefit from 2P advantages, ranging from diagnosis[21] to photodynamic therapy[22] to localized photorelease of active molecules[23] to image guided surgery.[24] In addition, nanoparticles are typically brighter than molecular dyes as long as their fluorescence is maintained. In the pursuit of obtaining bright FONs displaying large 2PA cross sections and emitting at long wavelengths, two major aspects should be considered: tuning the photophysical properties of the composing dye and balancing the effects of nanoconfinement. In this respect, molecular dye-based FONs represent the ultimate confinement, such that the chromophores are in direct interaction with each other, with no spacing polymeric or inorganic matrix. Thus, while the elevated content of dye subunits per nanoparticle should favor brightness and photo-stability,[25] intermolecular interactions may modulate the properties of the confined dyes, often to the detriment of fluorescence emission.[26] Therefore, controlling the relative orientation of dyes upon aggregation within FONs is determinant. Moreover, multipolar (i.e., dipolar, quadrupolar, or octupolar) dyes are preferred to achieve large 2PA responses. Therefore, by influencing the self-orientation upon aggregation and polarization of dye subunits, electrostatic interactions between dyes are expected to play a major role in determining the optical properties of the resulting NPs. As an example, we reported earlier the molecular engineering of tailor-made dipolar dyes that yield NIR-emitting FONs showing giant 2P brightness (up to 5×10^5 GM).[27]

Regarding the applicability of FONs to biomedical use, it should be noted that the interplay between NPs and living tissues is not yet fully understood.[28] A common practice toward controlling this parameter is to coat the surface of NPs, typically with polymers or zwitterionic moieties.[29] Such coatings have several purposes. First, they lower the immediate colloidal and biocompatibility issues of, typically inorganic, water-insoluble NPs. While this configuration allows for a plethora of applications, it is difficult to envisage for clinical translation since the potential toxicity of the core remains unchanged. Consequently, even though systematic studies are still lacking in this field, organic nanoparticles are often seen as promising alternatives to their inorganic counterparts. Second, surface coating aims at modulating the fate of NPs, i.e., whether they are internalized by cells or remain in the extracellular space. On the one hand, NP internalization by target cells is required for localized intracellular action. Coating thus often serves as a backbone for conjugating targeting ligands to the NPs.[30] On the other hand, long circulation times of NPs in vivo are favorable for long-term effects. Coating thus also aims at making overall stealthy NPs, i.e., NPs that do not interact with cellular membranes.[31] This rather contradictory role for the coating to mediate both targeted cellular uptake and otherwise stealthy behavior complicates the design of biocompatible NPs.

Taking a different approach toward addressing nanobio interactions, we recently reported on the use of a quadrupolar red fluorescent dye that yields spontaneously stealthy FONs.[20] We hypothesized that the quadrupolar structure of the dye, combined with its bulkiness and strong hydrophobic character could be in part responsible for the stealthy behavior of its FONs. Adding to this interesting property, the quadrupolar design hints at the possibility that these FONs may also be strong 2P absorbers. In this paper, we present a series of related dyes tuned to emit in the R-NIR spectral region (up to ∼ 700 nm) by elongating the π-conjugated system. These dyes yield FONs displaying giant 2P brightness values (up $\sigma_2^{max} \Phi_f$ ∼ 5×10^5 GM). Moreover, three of the four dye designs result in FONs also displaying a stealthy behavior toward cellular membranes. To highlight that these FONs can be used for bioimaging, we further coated them with a positively charged polymer to induce their internalization in living cells. We thus achieve controlled cellular uptake of organic nanoparticles for NIR-to-NIR bioimaging.

■ METHODS

This section provides an overview of the preparation, characterization and use of FONs. Extended experimental procedures with detailed methodology are provided as Supporting Information.

Dye Synthesis. The Q_{BDF} and Q_{BDtF} dyes were synthesized as in Li et al.[32] following a three-step procedure: a reactive donor-fluorene intermediate and an acceptor-bridge inter-mediate were first synthesized and then reacted together by Suzuki coupling. The Q_{BDeF} dye was synthesized via a similar route finalized by a Sonogashira coupling. The synthesis of the Q_{BDvF} dye followed a two-step procedure: a reactive donor-fluorene-bridge intermediate was first synthesized and then reacted onto the acceptor by Heck coupling.

FONs Preparation and Characterization. FONs were prepared by nanoprecipitation, a process consisting of the rapid addition of a minute amount of stock dye solution in spectral grade THF into a large volume of deionized water (1% v/v). When applicable, the surface coating of the FONs was subsequently achieved by dropwise addition of an aqueous poly(allylamine hydrochloride) (PAH) solution (1% v/v). FONs morphology was observed by transmission electron microscopy (Hitachi H7650) and their zeta potential determined on a nanoparticle analyzer (SZ-100 Horiba). Lifetime measurements were performed in the time-correlated

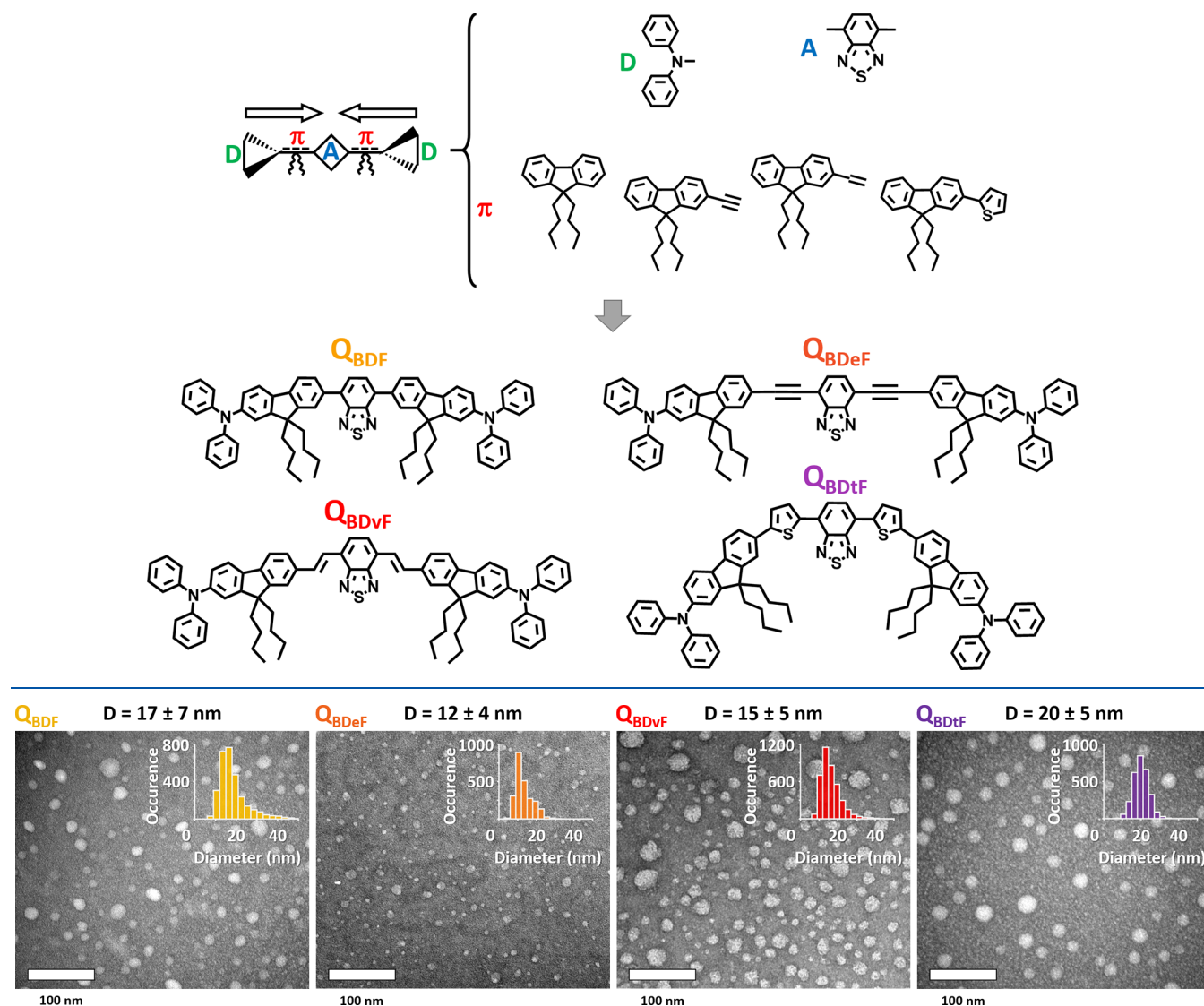**Scheme 1. Molecular Design of 2P Absorbing R-NIR-Emitting Dyes**

Figure 1. Representative transmission electron microscopy images of FONs made from quadrupolar dye subunits. Size distributions are provided by inset histograms obtained from populations of 3004, 2403, 3961, and 2878 objects, respectively.

single photon counting (TCSPC) configuration on a Fluorolog spectrofluorometer (Horiba).

Spectroscopy. 1P absorbance data were acquired on a UV/vis spectrophotometer (JASCO V-670). Thanks to the emissive properties of our dyes, 2P cross sections were determined using the 2P excitation fluorescence (TPEF) method. 2P absorbance data were acquired on an in-house setup using a Ti:sapphire oscillator (Coherent chameleon, Nd:YVO4, 140 fs, 80 MHz), a 10X objective (Provider, NA 0.25), and a compact CCD spectrometer (BWTek BTC112E). Emission data were acquired on a Fluoromax-4 spectrofluorometer (Horiba). Molar extinction coefficients, 2PA cross sections, and brightness values provided in the following tables and figures refer either to the molecular characteristics (Φ_f, σ_2) or to the FONs characteristics ($\Phi_{f,FONs}$, $\sigma_{2,FONs}$).

Cellular Imaging. FONs were incubated on Cos7 cells (1% v/v) for 24 h in serum-supplemented DMEM and washed with PBS prior to imaging. 1P imaging was achieved in the scanning-confocal configuration while 2P imaging was

performed on the same setup using a pulsed Mai-Tai excitation laser and an opened emission pinhole.

RESULTS AND DISCUSSION

Dye Design. The chromophores designed to yield stealthy, 2P-responsive, R-NIR-emitting FONs share a quadrupolar scheme (D−π−A−π−D). This symmetry was rationally introduced for two reasons. First because quadrupolar schemes favor large 2P absorption.[33] Second because it was meant to circumvent antiparallel arrangement of dipolar dyes driven by dipole−dipole interactions, which is deleterious to both fluorescence and 2PA.[34] As previously described for the Q_{BDF} dye,[20] the quadrupolar dyes display a benzothiadiazole (BDTA) acceptor moiety at their center, propeller-shaped diphenylamine donor moieties at their ends, and two alkylated fluorene motifs as hydrophobic, conjugated connectors linking the donors with the acceptor. The aim of choosing bulky propeller-shaped donor end groups and introducing steric hindrance with the alkyl chains was to hinder close π-stacking of the chromophores (i.e., formation of H-aggregates) within

nanoparticles, which would lead to vanishing fluorescence. From this common template, we modulated the connecting π-bridges, aiming to modulate the dyes' emission properties. The fluorenyl π-linkers were thus flanked with either ethynyl, vinyl, or thienyl motifs, resulting in the Q_{BDeF}, Q_{BDvF}, and Q_{BDtF} chromophores, respectively (Scheme 1). The good solubility in THF and insoluble character in water of these dyes make them good candidates for nanoprecipitation.[35]

FONs Preparation. Upon nanoprecipitation, Q_{BDF}, Q_{BDeF}, Q_{BDvF}, and Q_{BDtF} dyes all easily and rapidly yield transparent and colored aqueous colloidal solutions ranging from orange to pink. We confirmed the presence of spherical nanoparticles by transmission electron microscopy (TEM) (Figure 1). Interestingly, each chromophore spontaneously and reproducibly yields very small FONs of fixed median diameters with low polydispersity, ranging from 12 nm for Q_{BDeF} to 20 nm for Q_{BDtF}. In addition, FONs solutions display a highly negative potential around −65 mV (Table 1, Table S1).

Table 1. Structural Properties of FONs Made from Quadrupolar Dye Subunits

dye	$\varnothing_{TEM}$[a] [nm]	N[b]	ζ[c] [mV]
Q_{BDF}	17	1514	−65
Q_{BDeF}	12	509	−67
Q_{BDvF}	15	989	−62
Q_{BDtF}	20	2124	−63

[a]Dry diameter determined by transmission electron microscopy. [b]Number of dye subunits per nanoparticle calculated from $\varnothing_{TEM}$ assuming a density of 1. [c]Zeta potential.

Optical Properties. The spectral properties of dyes and FONs were characterized to determine the influence of the molecular structure and the effects of nanoconfinement on the optical properties of the resulting nanoparticles. Results are provided in Table 2 and Figure 2.

Linear Optical Properties in Solution. By selecting conjugated connectors of various natures, we manipulated the periphery-to-core intramolecular charge transfer (ICT) already present in Q_{BDF} in order to influence the photophysical properties of the new dyes. Elongating the π-bridges aimed at favoring red-shifted absorption and emission. We indeed observe the anticipated bathochromic shift in absorption for all three novels designs (Figure 2A). Moreover, we notice a marked increase (∼+50%) in their molar attenuation coefficient values as compared to the original Q_{BDF} template (Table 2). Interestingly, Q_{BDvF} and Q_{BDtF} dyes also display the awaited red shift in emission and exhibit quantum yield values of 0.6 and 0.4, gradually decreasing in accordance with the red-shifted emission.[36] Q_{BDeF}, however, behaves differently such that its emission in THF is more red-shifted (Figure 2A) and its fluorescence quantum yield is surprisingly low as compared to those of other derivatives (Table 2). We hypothesized that this specific behavior could be ascribed to the formation of a Twisted Intramolecular Charge Transfer (TICT) state[37] or to Photoinduced Electron Transfer (PET).[38] When dissolved in solvents of various polarities (Figure S1), the dyes do not display a marked shift in their ICT absorption band, underlying the neutral nature of the ground state of these symmetrical quadrupoles. In contrast, the emission spectra of

Table 2. 1P and 2P Optical Properties of Quadrupolar Dyes in THF and as FONs Subunits

dye		λ_{max}^{1P}[a] [nm]	ε^{max}[b] [10^4 M^{-1} cm^{-1}]	λ_{em}[c] [nm]	Φ_f[d] (%)	$2\lambda_{max}^{1P}$[e] [nm]	λ_{max}^{2P}[f] [nm]	σ_2^{max}[g] [10^3 GM]
Q_{BDF}	in THF	450	3.0	628	66	900	880	0.2
		338	4.9				820	0.8
		313	4.8					
	in FONs	458	2.5	591	30	916	880	0.5
		343	5.0				840	1.2
		321	5.0					
Q_{BDeF}	in THF	474	4.2	688	14	948	930	0.5
		369	5.7				880	1.5
		313	3.9				820	1.9
	in FONs	480	3.3	623	4	960	930	0.7
		371	5.3				890	1.3
		316	4.0				840	1.1
Q_{BDvF}	in THF	507	4.9	646	55	1014	930	0.7
		376	5.9				880	1.8
		311	4.0				820	2.4
	in FONs	505	4.1	646	2	1010	950	1.3
		370	6.9				910	1.7
		316	5.5				830	1.9
Q_{BDtF}	in THF	528	4.6	674	43	1056	980	0.6
		383	7.5				930	1.1
							890	2.2
		308	3.8				840	2.2
	in FONs	532	3.8	689	8	1064	950	1.6
		383	7.2				920	2.2
		311	4.5				890	2.4
							840	2.4

[a]Absorption maxima wavelengths under 1P excitation. [b]Molar extinction coefficient of the dye at λ_{max}^{1P}. [c]Emission maximum wavelength. [d]Fluorescence quantum yield. [e]Twice λ_{max}^{1P} corresponding to the low-energy (ICT) absorption band. [f]Absorption maxima wavelengths under 2P excitation. [g]2PA cross-section of the dye at λ_{max}^{2P}.
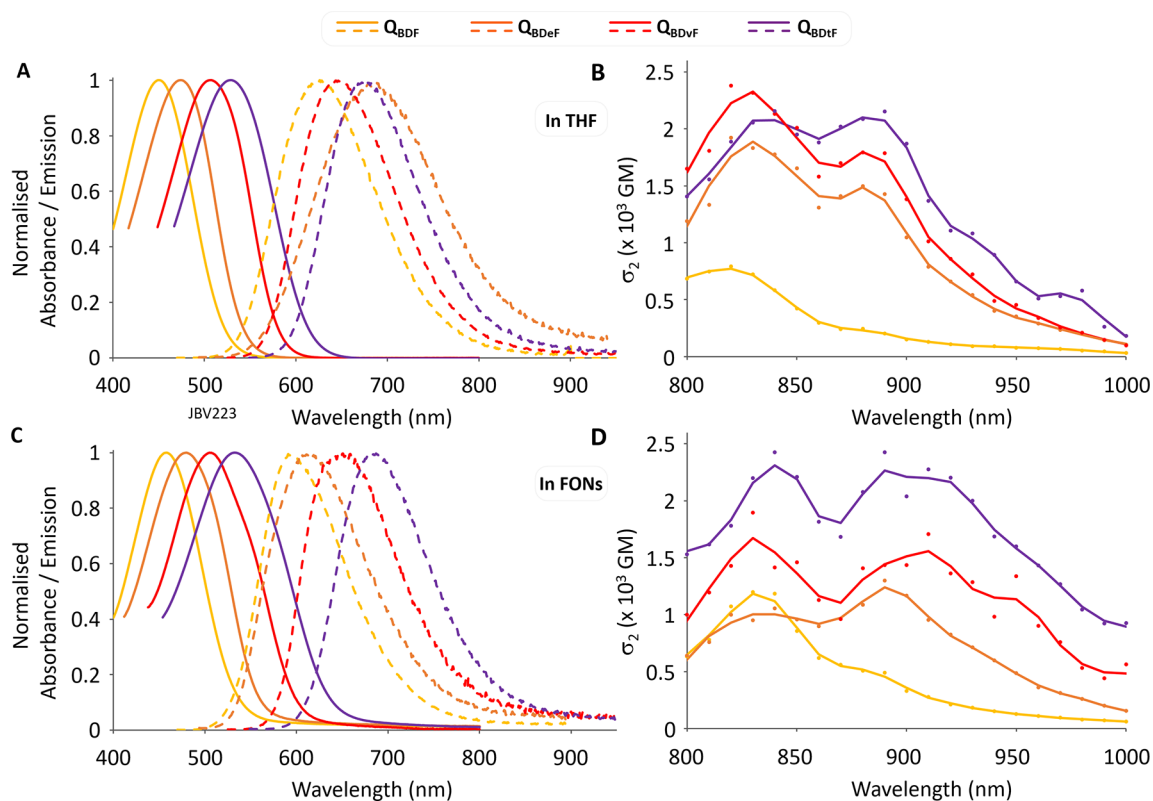
Figure 2. Optical properties of the dyes in THF (top) and in FONs (bottom). (A−C) Overlapped normalized 1P absorption (solid lines) and emission (dashed lines) spectra. (B−D) Overlapped 2P absorption spectra.

all four compounds show a pronounced red shift with increasing solvent polarity, suggesting that symmetry breaking occurs in in the excited state leading to a polarized emitting state.[39,40] Interestingly, we note from these experiments that Q_{BDeF} emission is much more sensitive to solvent polarity than other dyes (Table S2). However, as it is not sensitive to the viscosity of the solvent (Figure S2), the TICT hypothesis can be ruled out. This result thus argues in favor of intramolecular PET competing with fluorescence emission in THF and being responsible for the low fluorescence quantum yield of this compound. Taken together, these dyes display interesting R-NIR emission upon visible excitation in low to medium polarity solvents, some of which with relatively high quantum yields.

Nonlinear Optical Properties in Solution. The four dyes display interestingly high σ_2^{max} values in the NIR region ranging from 1 to 2×10^3 GM in THF (Table 2, Figure 2). We note that these values are higher than those reported for shorter analogous D−A−D derivatives,[41] as well as for similar derivatives bearing acceptor end-groups[42] instead of the strong donating end-groups used here, or for proquinoidal D−A−D or D−A−D−A−D derivatives built from BDTA units.[43] As expected from the quadrupolar nature of the dyes, the 2PA peaks are markedly blue-shifted as compared to twice the wavelength of the 1P absorption peak (Table 2 and Figure S3). Yet we observe a shoulder in the 2PA spectra, indicating that the lowest 1P excited state is also partly 2P allowed. This observation may be related to the conformational flexibility and V-shape of the dyes,[44] which are not purely linear quadrupoles. The dipolar component of the 2PA signal results in sizable 2PA cross-section values (200−700 GM) for Q_{BDF}, Q_{BDeF}, and Q_{BDvF} dyes around 880 or 930 nm nm, respectively.

The V-shape of Q_{BDtF} even leads to the appearance of a definite 2PA band located at 980 nm and peaking at ∼600 GM, a promising property for 2P microscopy of thick biological samples. Moreover, the extended conjugation induces a red shift (from 820 nm in Q_{BDF} to 880 or 890 nm in the other dyes) and marked increase (from 800 GM in Q_{BDF} to 1500, 1800, and 2200 GM in Q_{BDeF}, Q_{BDvF}, and Q_{BDtF}, respectively) in the 2PA peak corresponding to the strongly 2P-allowed excited state (quadrupolar component). Finally, we note the appearance of an additional, higher energy band in the 2PA spectra of extended dyes. Ideally located around the maximum excitation achievable with a Ti:sapphire laser commonly used for 2P microscopy, this 820−840 nm band leads to 2PA responses about 2−3-fold higher in the elongated dyes than in Q_{BDF} at the same wavelength (i.e., 1900, 2400, and 2200 GM, respectively, for dyes Q_{BDeF}, Q_{BDvF}, and Q_{BDtF}).

Confinement Effects on Linear Optical Properties. As dye molecules self-assemble into nanoparticles upon nanoprecipitation in water, specific optical properties may arise, depending on the relative positioning of the dyes and their interchromophoric interactions within aggregates. These may include excitonic coupling, electrostatic interactions and charge transfer interactions.[45−48] All four dyes remain strong absorbers as dye subunits within FONs (Table 1). Following the trend observed in solution under 1P excitation, elongating the conjugation bridge induces a bathochromic shift of the ICT absorption band in FONs (Figure 2C). Similarly, we note a comparable ∼+50%−100% increase in the molar absorption coefficient values of Q_{BDeF}, Q_{BDvF}, and Q_{BDtF} dyes in FONs as compared to Q_{BDF}.

We also notice that these ε^{max} values decrease upon aggregation (∼−20%), with the exception of that of Q_{BDvF}
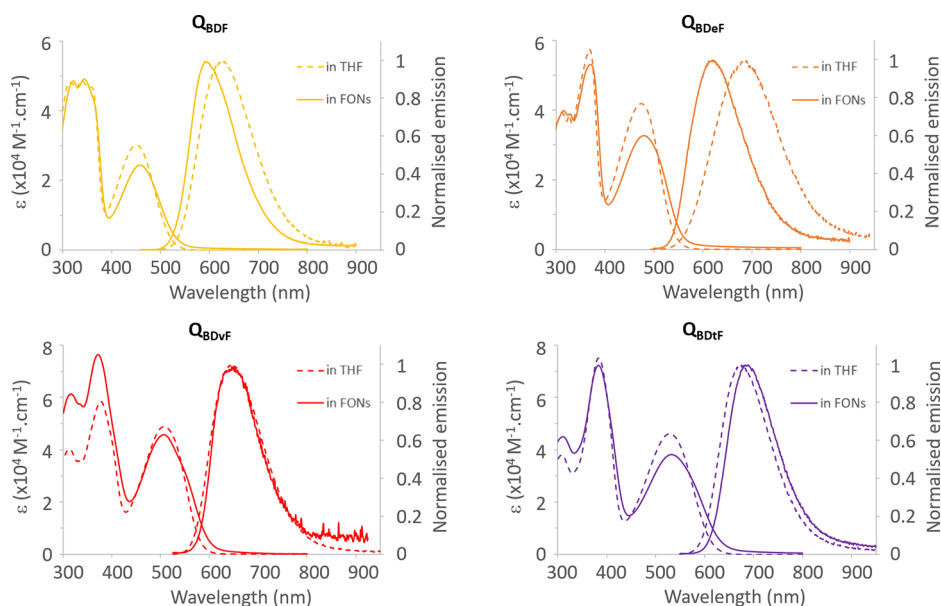
Figure 3. Linear properties of the dyes in THF (dashed lines) and in FONs (solid lines).
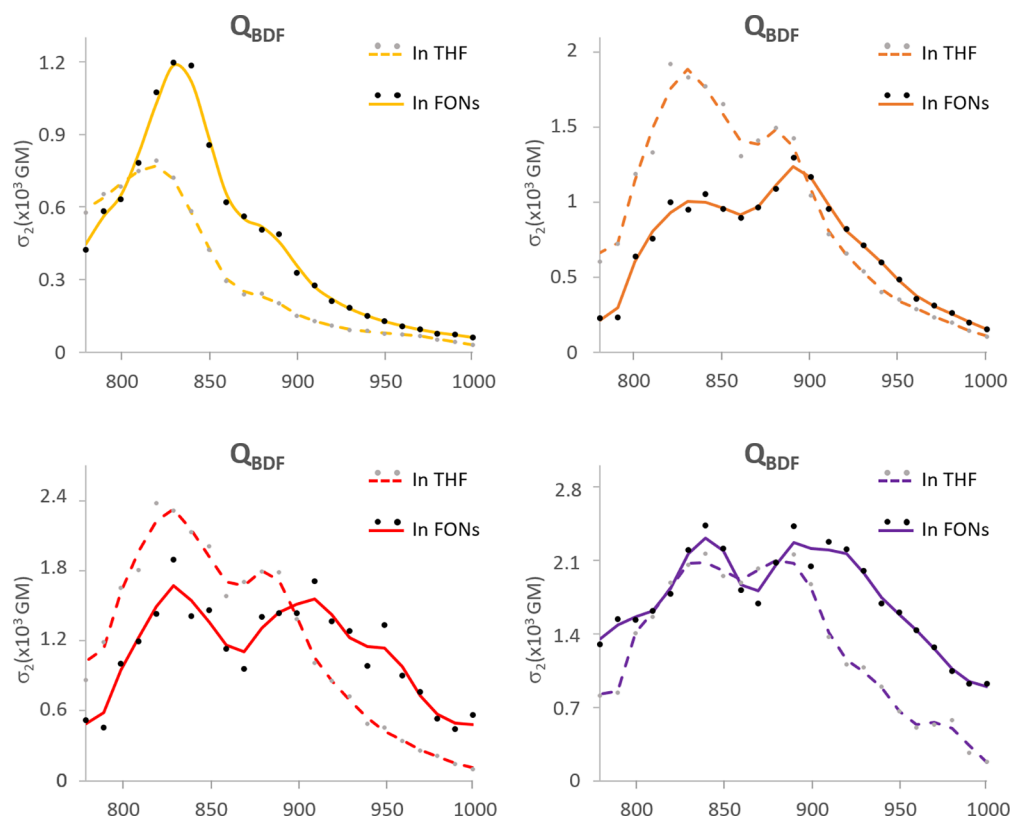

Figure 4. Nonlinear properties of the dyes in THF (dashed lines) and in FONs (solid lines).

which remains almost unchanged (Figure 3). Additionally, while the ICT bands of Q_{BDF} dyes in THF and in FONs have similar full-widths at half-maximum (fwhm), we note a slight flattening and broadening of the low energy ICT bands, with the appearance of a red shoulder in the case of Q_{BDvF} and Q_{BDtF}. Regarding emission, contrary to what was observed in THF, the emission maxima of dyes in FONs follow the trend of the absorption bands (Figure 2). In other words, Q_{BDeF} now behaves as anticipated, with an emission maximum lying in between the peaks of the shorter Q_{BDF} dye and the more

flexible Q_{BDvF} dye. We also note that all dyes do not show similar band shifts upon aggregation. While Q_{BDF} and Q_{BDeF} dyes emissions are blue-shifted in FONs as compared to in THF, Q_{BDvF} dyes emit at the same wavelength, and the Q_{BDtF} dyes emissions are red-shifted (Figure 3). The fluorescence quantum yield of the dyes significantly decreases as compared to those of the dyes dissolved in low to medium polarity solvents (Table S2). This can be ascribed to both a decrease of the radiative decay rate and an increase in the nonradiative decay rate. This loss may be ascribed to both interchromo-

Table 3. Optical Properties of the FONs Made from Quadrupolar Dye Subunits

dye	λ_{max}^{1P} [nm][a]	λ_{em}^{b} [nm]	ε_{FONs}^{c} [10^7 M^{-1} cm^{-1}]	$\varepsilon_{FONs}\Phi_f^{d}$ [$10^6 M^{-1}$ cm^{-1}]	λ_{max}^{2P} [nm][e]	$\sigma_{2,FONs}^{f}$ [10^6 GM]	$\sigma_{2,FONs}\Phi_f^{g}$ [10^5 GM]
Q_{BDF}	458	591	3.8	11.1	840	1.8	5.4
Q_{BDeF}	480	623	1.7	0.7	890	0.7	0.3
Q_{BDvF}	505	646	4.1	0.9	890	1.4	0.3
Q_{BDtF}	532	689	8.1	6.5	890	5.2	4.1

[a]Absorption maximum wavelength corresponding to the low-energy (ICT) band under 1P excitation. [b]Emission maximum wavelength. [c]Estimated molar extinction coefficient of FONs at λ_{max}^{1P} considering N dye molecules per FON (see Table 1). [d]Estimated 1P brightness of FONs. [e]Absorption maximum wavelength under 2P excitation. [f]Estimated cross-section of FONs at λ_{max}^{2P} considering N dye molecules per FON. [g]Estimated 2P brightness of FONs.

phoric interactions (leading to a reduction of the radiative rate) and additional nonradiative decay process favored by water molecules bound to the FONs surface. Yet, we stress that the fluorescence quantum yield values (2% to 30%) remain substantial for R-NIR-emitting nanoparticles in water in the absence of protective additives. Interestingly, while the quantum yield values of Q_{BDF}, Q_{BDeF}, and Q_{BDvF} dyes decrease with increased conjugation, the quantum yield of Q_{BDtF} in FONs remains larger than that of the other extended dyes (i.e., 8%). As a result, the FONs made from Q_{BDtF} dyes show both the most red-shifted and most intense fluorescence of the elongated dyes, suggesting a more favorable packing within FONs.[45,46] This is consistent with the evolution of the radiative rate values (Table S2).

Confinement Effects on Nonlinear Optical Properties. All dyes retain very large 2PA responses in the NIR region within FONs (Table 2, Figure 2D). Similarly to what was observed in solution, the 2PA responses significantly increase with conjugation, with Q_{BDF} having the lowest peak 2PA cross-section, Q_{BDtF} having the highest, and Q_{BDeF} and Q_{BDvF} having intermediate values. Yet a more detailed observation shows that the nanoconfinement of the dyes into nanoparticles affects their 2PA spectra, in a different manner depending on the structure of the dye (Figure 4). Most interestingly, Q_{BDF} displays an increase of its σ_2^{max} value at 820 nm by ∼50% along with a slight red shift (from 820 to 840 nm). Interestingly, its low energy 2PA band located at 880 nm corresponding to the lowest 1P allowed excited state (dipolar component) is even more impacted with an increase by ∼100% (Table 1). This cooperative enhancement may be tentatively ascribed to electrostatic interchromophoric inter-actions whose effects depend on the relative positioning of the quadrupolar dyes within the aggregate In contrast, the quadrupolar component of the 2PA response of Q_{BDeF}, Q_{BDvF}, and Q_{BDtF} dyes (peaking around 880−910 nm) remains mostly unaffected with variations lying within the experimental error. In contrast, a decrease of the highest energy 2PA band located at 820−840 nm may is observed for dye Q_{BDeF} while no meaningful differences are observed for extended dyes Q_{BDvF} and Q_{BDtF}. For these two extended dyes, the main effect of confinement is a spectral broadening of the 2PA bands and a pronounced increase of the 2PA response of the low energy sub-band located around 950 nm (Figure 4). As a result, Q_{BDvF} and Q_{BDtF} maintain high 2PA responses (>1000 GM) at 950 nm. From a practical point of view, this is of major interest for bioimaging purposes as it allows for improved collection and spectral discrimination of the fluorescence signal by operating at 2P excitation wavelengths away from the R-NIR emission.

FONs Brightness and Stability. While studying the optical properties of dyes in solution and in FONs help us understand the effects of confinement, the properties of the

FONs themselves, as a collection of a multitude of dyes, should be considered for applications. The brightness of FONs is described as the product of their absorption capacity (ε or σ_2) and their emissive capacity (Φ_f). As shown in Table 3, FONs exhibit giant molar extinction coefficients (with ε_{FONs} values in the 10^7 M^{-1} cm^{-1} range) and 2PA cross sections (with $\sigma_{2,FONs}$ values in the 10^6 GM range), thanks to the high number of dyes that are accommodated per nanoparticle ranging from a few hundreds to a couple thousands (Table 1).

We had previously reported that the remarkable absorption and significant fluorescence quantum yield of Q_{BDF} let its FONs reach a giant 1P brightness of 1×10^7 M^{-1} cm^{-1}.[20] We now report that these FONs also display a huge 2P brightness of 6×10^5 GM. Interestingly, the excellent properties of Q_{BDtF} FONs described above make them our second brightest probe, with the foremost advantage that both its absorption and emission are red-shifted as compared to Q_{BDF}. In addition, Q_{BDtF} FONs retain huge 2P brightness at 950 nm (3×10^5 GM) revealing the potential for NIR-to-NIR imaging in thick biological samples. Q_{BDeF} and Q_{BDvF} display lower 1P and 2P brightness values, in relation to their smaller size and lower fluorescence quantum yields (Figure S4). Overall, the bottom-up molecular engineering based on the use of quadrupolar dyes derived from the Q_{BDF} structure as FONs subunits proved to be even more successful than an earlier study based on dipolar dyes,[27] with, notably, Q_{BDtF} FONs reaching a similar 2P brightness as NIR-emitting FONs reported earlier[27] despite being twice as small. For comparison, red-emitting inorganic quantum dots, long considered the state-of-the-art in terms of probe brightness, display 10^6 M^{-1} cm^{-1} 1P brightness[49] and 10^4 GM 2P brightness[50] values in water. Among organic nanoparticles, polymeric red-emitting nanoparticles of small size (Ø < 30 nm) rarely reach 10^6 M^{-1} cm^{-1} 1P brightness[51] and 10^5 GM 2P brightness[51] values. Our FONs are thus closer to another family of all-organic, fluorescent nanoparticles referred to as AIE-dots. Most R-NIR-emitting AIE-dots display 1P brightness comparable to QDs (and exceptionally up to 10^7 M^{-1} cm^{-1})[52] and 10^5 GM 2P brightness values.[53] However, the formulation of these dots requires polymeric surfactants and the resulting nanoparticles are usually larger (Ø > 30 nm). The FONs presented in this study therefore compare positively to other types of nanoparticles in terms of size, brightness, and simplicity.

Finally, FONs should be stable in time to be easily usable. The highly negative zeta potential of the solution is indicative that these FONs may be colloidally stable, as electrostatic repulsion between particles helps prevent them from aggregating. We found that Q_{BDF}, Q_{BDeF}, and Q_{BDtF} FONs absorption remains virtually unchanged over a month (Figure S5). Namely, we observe no setting and no appearance of a background scattering signal suggestive of the formation of
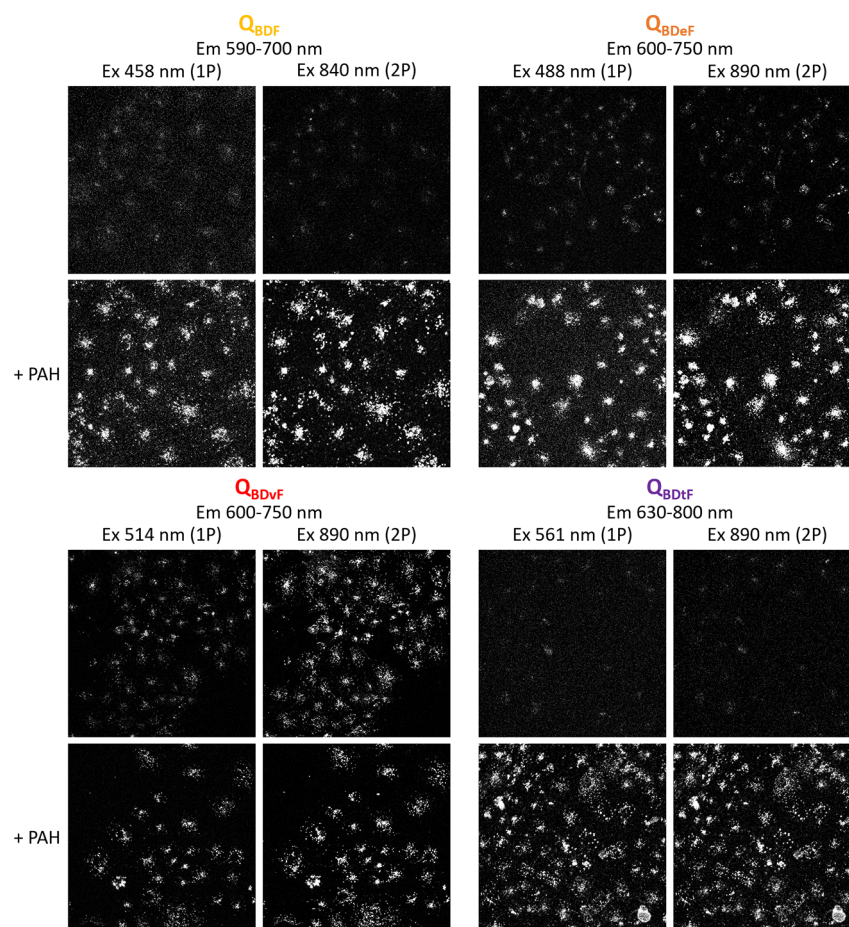
Figure 5. Interplay between FONs and living cells. For each type of FONs, representative 1P (left) and 2P (right) fluorescence images of bare (top) and PAH-coated (bottom) FONs incubated for 24h on Cos7 cells (1% v/v in cell culture medium) are provided. Maximal projections of z-stack images are displayed. Excitation wavelengths and emission detection ranges are indicated for each condition.

microagglomerates, nor any decrease in the intensity of the ICT absorption band. Oppositely, Q_{BDvF} FONs appear surprisingly less stable, with a gradual decrease of the ICT band over time. This striking difference suggests that the structuration of the chromophores at the surface of the FONs markedly differs for this dye in such a way that nanoparticles are structurally much less stable at the interface with water. In other words, the interaction energy of a single Q_{BDvF} dye with the FONs surface appears as lowered compared to the other dyes, favoring either exchange with the bulk aqueous phase or with other nanoparticles upon contact. This finding emphasizes the critical point that a subtle change of the molecular structure of the dyes may significantly affect the colloidal stability of its FONs.[54] Emission is slightly more affected than absorption for all chromophores, with Q_{BDF} and Q_{BDeF} FONs quantum yields decreasing by about 30% over a month, and that of Q_{BDtF} FONs by about 50%. This indicates that place exchange leading to surface defects[55] acting as fluorescence traps is a slow process and suggests that in comparison dyes Q_{BDF}, Q_{BDeF}, and Q_{BDtF} show larger interaction energy with the surface.

FONs Behavior in a Cellular Environment Monitored by Fluorescence Imaging. Building upon the promising properties of these FONs, i.e., red-shifted emission and high 1P and 2P brightness, we next investigated their usability for cellular imaging with two questions in mind: (i) Do the three novel dye designs Q_{BDeF}, Q_{BDvF}, and Q_{BDtF} yield stealthy FONs

as the Q_{BDF} dye does? (ii) Can stealthy FONs be functionalized for controlled intracellular delivery? Moreover, we wanted to assess whether these FONs were compatible with 2P microscopy, as their optical properties would suggest.

By incubating Cos7 cells with FONs for 24 h and imaging them under a 1P confocal microscope, we confirmed that Q_{BDF} FONs do not internalize or stick to membranes of living cells. This result is in accordance with their stealthy behavior previously observed toward HeLa cells.[20] Most interestingly, we observed the same lack of interactions for Q_{BDtF} FONs. Q_{BDvF} FONs, on the other hand, could readily be observed accumulated inside of cells. An intermediate behavior was observed for Q_{BDeF} FONs, which were detectably internalized but at lower levels than Q_{BDvF} FONs (Figure 5, upper panels). This suggests that our rationale for dye design, i.e., elongated quadrupoles with pendant hydrophobic chains close to the end of the dyes, indeed tends to yield stealthy FONs. Interestingly, other factors appear to come to play to rationally engineer this property and control its tunability. Notably, it appears that the rigidity of the dye backbone may be of importance, as the introduction of a flexible double bond in the Q_{BDvF} dye induces the internalization of Q_{BDvF} FONs. This again points to a different surface organization of the dyes as compared to the other chromophores, presumably responsible for both the uptake of these FONs by cells and their strikingly reduced colloidal stability. Further complementary studies dedicated to understanding these different organizations will be of the

highest interest in view of fully controlling the nanobio interface.

The original spontaneous stealth property of Q_{BDF}, Q_{BDeF}, and Q_{BDtF} FONs opens the possibility of controlling their intracellular delivery via surface functionalization. We reasoned that shielding their surface would modulate their interactions with cells. We chose poly(allylamine hydrochloride) (PAH) as a coating polymer, both because its cationic nature would allow it to electrostatically interact with the negatively charged FONs and because it is known to enhance nanoparticle intracellular delivery.[56] Coating was achieved by simple dropwise addition of PAH into the FONs solution under agitation and confirmed by observing the reversal of the solution's zeta potential (Table S4) Of note, the PAH coating did not modulate the in vitro optical and colloidal properties of FONs (Figure S6). When incubated under the same conditions as bare FONs, all four PAH-coated FONs were strongly taken up by Cos7 cells (Figure 5, lower panels). Importantly, Q_{BDF}@PAH and Q_{BDtF}@PAH FONs readily internalized although their bare counterparts did not. Notably, we observed no further increase in the internalization of Q_{BDvF}@PAH FONs as compared to bare Q_{BDvF} FONs. Oppositely, Q_{BDeF}@PAH FONs were clearly more internalized than bare Q_{BDeF} FONs. This suggests that cellular uptake of bare Q_{BDvF} FONs is already rapid and maximal whereas the slight uptake of bare Q_{BDeF} FONs is slow and can be enhanced by PAH coating. Finally, the strong signal originating from internalized FONs allowed us to confirm that all four types of FONs can be readily imaged under 2P excitation well within the optical transparency window. Our dye designs therefore yield a novel class of bright, 2P responsive, fluorescent nanoparticles. In this regard, the 890 to 950 nm-absorbing, 700 nm-emitting, and very stealthy Q_{BDtF} FONs appear as ideal candidates for NIR-to-NIR bioimaging with organic nanoprobes.

CONCLUSIONS

We have described and discussed the design, optical properties, and bioimaging potential of a series of new R-NIR-emitting all-organic nanoparticles obtained by nanoprecipitation of quadrupolar dyes explicitly engineered to address two major properties relevant to biomedical applications: R-NIR absorption and emission, and reduced interactions with cells.

Starting from a previously described molecular template, recently shown to yield stealthy nanoparticles,[20] we tuned the photophysical properties of three dyes by modulating the nature, length, and rigidity of conjugated π-connectors between bulky diphenylamine donor groups and a benzothiadiazole acceptor core. We show that these modulations have successfully induced a hyperchromic and bathochromic shift as compared to the original Q_{BDF} design. We also demonstrate that these quadrupoles all possess significant 2PA capacities, with the prototypical Q_{BDF} dye even displaying aggregation induced enhancement of its 2PA cross sections in FONs while the two most extended dyes show definite 2PA spectral broadening in the 900−1000 nm spectral region. The obtained FONs therefore absorb and emit within the biological transparency window. Moreover, they display remarkable 1P and 2P brightness values. Interestingly, the present study also demonstrates that the nature of the conjugated linkers has a significant influence on the effect of nanoconfinement on the optical properties. As a result, the Q_{BDtF} dye leads to NIR-emitting FONs showing both the more red-shifted and more intense NIR emission, the largest brightness and enhanced

2PA in the 900−950 nm range. In contrast, the R-NIR-emitting FONs made from the Q_{BDvF} dye show lower fluorescence and even more importantly strikingly reduced colloidal stability that reveals an additional role of the flexible π-bridges on the structuration of the FONs surface. Taken together, these properties allow FONs to compete with the current state of the art, especially for such small nanoprobes of no more than 20 nm in diameter.

In addition to these remarkable optical properties, we found that three of the four dyes derived from this template yield FONs that spontaneously minimally interact with cellular membranes. Interestingly, the most fluorescent and colloidally stable FONs (i.e., made from orange/red-emitting Q_{BDF} and NIR-emitting Q_{BDtF}) were also the most stealthy FONs. As these first two parameters can be engineered by a bottom-up approach, this observation strongly suggests that controlling the nanobio interface can be rationally addressed too. The present study therefore represents a first step toward this goal in the field of single component organic nanoparticles. We hypothesize that the nano-organization of the dyes at the surface is key to addressing this issue and expect that detailed studies of the molecular arrangements occurring at the interface will be of the highest interest to further explore this concept. In that regard, complementary theoretical studies involving physical models[47] and molecular dynamics simulations combined with quantum chemical calculations to characterize the effect of self-assembly on optical properties[57] will be critical to advance our understanding of the linear and nonlinear photophysical properties of these nano-objects. In addition, further experimental and spectroscopic studies[55] will be needed to get better insight into the nature of their surface.

Finally, we have shown that the surface of FONs can be noncovalently functionalized with a positively charged polymer to induce their cellular internalization. Under these conditions, FONs were clearly visible under 2P excitation, confirming our in vitro results and pointing to a potential use for deep tissue bioimaging. In this context, we believe that Q_{BDtF} FONs represent the best candidates as promising all-organic, spontaneously stealthy, NIR-to-NIR bioimaging nanoprobes.

ASSOCIATED CONTENT

Ⓢ Supporting Information

The Supporting Information is available free of charge at https://pubs.acs.org/doi/10.1021/acs.jpcc.1c07831.

> Materials and methods, characterization data, tables of TEM data, decay rates, reversal of surface potentials, figures of absorption and emission spectra and brightness (PDF)

AUTHOR INFORMATION

Corresponding Author

Mireille Blanchard-Desce − *Université Bordeaux, CNRS, Bordeaux INP, ISM, UMR 5255, F-33400 Talence, France;* ⓞ orcid.org/0000-0002-1572-9545; Email: mireille.blanchard-desce@u-bordeaux.fr

Authors

Paolo Pagano − *Université Bordeaux, CNRS, Bordeaux INP, ISM, UMR 5255, F-33400 Talence, France*

Morgane Rosendale − *Université Bordeaux, CNRS, Bordeaux INP, ISM, UMR 5255, F-33400 Talence, France*

Jonathan Daniel − *Université Bordeaux, CNRS, Bordeaux INP, ISM, UMR 5255, F-33400 Talence, France*

Jean-Baptiste Verlhac − *Université Bordeaux, CNRS, Bordeaux INP, ISM, UMR 5255, F-33400 Talence, France*

Complete contact information is available at:
https://pubs.acs.org/10.1021/acs.jpcc.1c07831

Author Contributions

[‡]These authors contributed equally

Notes

The authors declare no competing financial interest.

■ REFERENCES

(1) Frangioni, J. V. In Vivo Near-Infrared Fluorescence Imaging. *Curr. Opin. Chem. Biol.* **2003**, *7* (5), 626−634.

(2) Jacques, S. L. Optical Properties of Biological Tissues: A Review. *Phys. Med. Biol.* **2013**, *58* (11), R37−R61.

(3) Zipfel, W. R.; Williams, R. M.; Webb, W. W. Nonlinear Magic: Multiphoton Microscopy in the Biosciences. *Nat. Biotechnol.* **2003**, *21* (11), 1369−1377.

(4) Ricard, C.; Arroyo, E. D.; He, C. X.; Portera-Cailliau, C.; Lepousez, G.; Canepari, M.; Fiole, D. Two-Photon Probes for in Vivo Multicolor Microscopy of the Structure and Signals of Brain Cells. *Brain Struct. Funct.* **2018**, *223* (7), 3011−3043.

(5) Terenziani, F.; Katan, C.; Badaeva, E.; Tretiak, S.; Blanchard-Desce, M. Enhanced Two-Photon Absorption of Organic Chromophores: Theoretical and Experimental Assessments. *Adv. Mater.* **2008**, *20* (24), 4641−4678.

(6) Kim, H. M.; Cho, B. R. Two-Photon Materials with Large Two-Photon Cross Sections. Structure−Property Relationship. *Chem. Commun.* **2009**, *2*, 153−164.

(7) Pawlicki, M.; Collins, H. A.; Denning, R. G.; Anderson, H. L. Two-Photon Absorption and the Design of Two-Photon Dyes. *Angew. Chem., Int. Ed.* **2009**, *48* (18), 3244−3266.

(8) Reinhardt, B. A.; Brott, L. L.; Clarson, S. J.; Dillard, A. G.; Bhatt, J. C.; Kannan, R.; Yuan, L.; He, G. S.; Prasad, P. N. Highly Active Two-Photon Dyes: Design, Synthesis, and Characterization toward Application. *Chem. Mater.* **1998**, *10* (7), 1863−1874.

(9) Jun, Y. W.; Kim, H. R.; Reo, Y. J.; Dai, M.; Ahn, K. H. Addressing the Autofluorescence Issue in Deep Tissue Imaging by Two-Photon Microscopy: The Significance of Far-Red Emitting Dyes. *Chem. Sci.* **2017**, *8* (11), 7696−7704.

(10) Pascal, S.; David, S.; Andraud, C.; Maury, O. Near-Infrared Dyes for Two-Photon Absorption in the Short-Wavelength Infrared: Strategies towards Optical Power Limiting. *Chem. Soc. Rev.* **2021**, *50* (11), 6613−6658.

(11) Prévot, G.; Bsaibess, T.; Daniel, J.; Genevois, C.; Clermont, G.; Sasaki, I.; Marais, S.; Couillaud, F.; Crauste-Manciet, S.; Blanchard-Desce, M. Multimodal Optical Contrast Agents as New Tools for Monitoring and Tuning Nanoemulsion Internalisation into Cancer Cells. From Live Cell Imaging to in Vivo Imaging of Tumours. *Nanoscale Adv.* **2020**, *2* (4), 1590−1602.

(12) *Single Organic Nanoparticles*; Masuhara, H., Nakanishi, H., Sasaki, K., Eds.; NanoScience and Technology; Avouris, P., von Klitzing, K., Sakaki, H., Wiesendanger, R., Series Eds.; Springer Berlin Heidelberg: Berlin, Heidelberg, 2003; DOI: 10.1007/978-3-642-55545-9.

(13) Fery-Forgues, S. Fluorescent Organic Nanocrystals and Non-Doped Nanoparticles for Biological Applications. *Nanoscale* **2013**, *5* (18), 8428.

(14) Fu, H.-B.; Yao, J.-N. Size Effects on the Optical Properties of Organic Nanoparticles. *J. Am. Chem. Soc.* **2001**, *123* (7), 1434−1439.

(15) Bhongale, C. J.; Chang, C.-W.; Lee, C.-S.; Diau, E. W.-G.; Hsu, C.-S. Relaxation Dynamics and Structural Characterization of Organic Nanoparticles with Enhanced Emission. *J. Phys. Chem. B* **2005**, *109* (28), 13472−13482.

(16) Abbel, R.; van der Weegen, R.; Meijer, E. W.; Schenning, A. P. H. J. Multicolour Self-Assembled Particles of Fluorene-Based Bolaamphiphiles. *Chem. Commun.* **2009**, *13*, 1697−1699.

(17) Ishow, E.; Brosseau, A.; Clavier, G.; Nakatani, K.; Tauc, P.; Fiorini-Debuisschert, C.; Neveu, S.; Sandre, O.; Léaustic, A. Multicolor Emission of Small Molecule-Based Amorphous Thin Films and Nanoparticles with a Single Excitation Wavelength. *Chem. Mater.* **2008**, *20* (21), 6597−6599.

(18) Parthasarathy, V.; Fery-Forgues, S.; Campioli, E.; Recher, G.; Terenziani, F.; Blanchard-Desce, M. Dipolar versus Octupolar Triphenylamine-Based Fluorescent Organic Nanoparticles as Brilliant One- and Two-Photon Emitters for (Bio)Imaging. *Small* **2011**, *7* (22), 3219−3229.

(19) Pennakalathil, J.; Jahja, E.; Ozdemir, E. S.; Konu, O.; Tuncel, D. Red Emitting, Cucurbituril-Capped, PH-Responsive Conjugated Oligomer-Based Nanoparticles for Drug Delivery and Cellular Imaging. *Biomacromolecules* **2014**, *15* (9), 3366−3374.

(20) Rosendale, M.; Flores, J.; Paviolo, C.; Pagano, P.; Daniel, J.; Ferreira, J.; Verlhac, J.-B.; Groc, L.; Cognet, L.; Blanchard-Desce, M. A Bottom-Up Approach to Red-Emitting Molecular-Based Nanoparticles with Natural Stealth Properties and Their Use for Single-Particle Tracking Deep in Brain Tissue. *Adv. Mater.* **2021**, *33* (22), 2006644.

(21) Perumal, V.; Sivakumar, P. M.; Zarrabi, A.; Muthupandian, S.; Vijayaraghavalu, S.; Sahoo, K.; Das, A.; Das, S.; Payyappilly, S. S.; Das, S. Near Infra-Red Polymeric Nanoparticle Based Optical Imaging in Cancer Diagnosis. *J. Photochem. Photobiol., B* **2019**, *199*, 111630.

(22) Bekmukhametova, A.; Ruprai, H.; Hook, J. M.; Mawad, D.; Houang, J.; Lauto, A. Photodynamic Therapy with Nanoparticles to Combat Microbial Infection and Resistance. *Nanoscale* **2020**, *12* (41), 21034−21059.

(23) Karimi, M.; Sahandi Zangabad, P.; Baghaee-Ravari, S.; Ghazadeh, M.; Mirshekari, H.; Hamblin, M. R. Smart Nanostructures for Cargo Delivery: Uncaging and Activating by Light. *J. Am. Chem. Soc.* **2017**, *139* (13), 4584−4610.

(24) Wojtynek, N. E.; Mohs, A. M. Image-Guided Tumor Surgery: The Emerging Role of Nanotechnology. *Wiley Interdisc. Rev.: Nanomed. Nanobiotechnol.* **2020**, *12* (4), No. e1624.

(25) Lou, X.; Zhao, Z.; Tang, B. Z. Organic Dots Based on AIEgens for Two-Photon Fluorescence Bioimaging. *Small* **2016**, *12* (47), 6430−6450.

(26) Li, Y.; Zhou, H.; Chen, J.; Anjum Shahzad, S.; Yu, C. Controlled Self-Assembly of Small Molecule Probes and the Related Applications in Bioanalysis. *Biosens. Bioelectron.* **2016**, *76*, 38−53.

(27) Mastrodonato, C.; Pagano, P.; Daniel, J.; Vaultier, M.; Blanchard-Desce, M. Molecular-Based Fluorescent Nanoparticles Built from Dedicated Dipolar Thienothiophene Dyes as Ultra-Bright Green to NIR Nanoemitters. *Molecules* 2016, *21* (9), 1227.

(28) Villanueva-Flores, F.; Castro-Lugo, A.; Ramírez, O. T.; Palomares, L. A. Understanding Cellular Interactions with Nanomaterials: Towards a Rational Design of Medical Nanodevices. *Nanotechnology* 2020, *31* (13), 132002.

(29) Schubert, J.; Chanana, M. Coating Matters: Review on Colloidal Stability of Nanoparticles with Biocompatible Coatings in Biological Media, Living Cells and Organisms. *Curr. Med. Chem.* 2018, *25* (35), 4553−4586.

(30) Yoo, J.; Park, C.; Yi, G.; Lee, D.; Koo, H. Active Targeting Strategies Using Biological Ligands for Nanoparticle Drug Delivery Systems. *Cancers* 2019, *11* (5), 640.

(31) Fam, S. Y.; Chee, C. F.; Yong, C. Y.; Ho, K. L.; Mariatulqabtiah, A. R.; Tan, W. S. Stealth Coating of Nanoparticles in Drug-Delivery Systems. *Nanomaterials* 2020, *10* (4), 787.

(32) Li, Z. H.; Wong, M. S.; Fukutani, H.; Tao, Y. Full Emission Color Tuning in Bis-Dipolar Diphenylamino-Endcapped Oligoarylfluorenes. *Chem. Mater.* 2005, *17* (20), 5032−5040.

(33) Albota, M.; Beljonne, D.; Brédas, J.-L.; Ehrlich, J. E.; Fu, J.-Y.; Heikal, A. A.; Hess, S. E.; Kogej, T.; Levin, M. D.; Marder, S. R.; McCord-Maughon, D.; Perry, J. W.; Röckel, H.; Rumi, M.; Subramaniam, G.; Webb, W. W.; Wu, X.-L.; Xu, C. Design of Organic Molecules with Large Two-Photon Absorption Cross Sections. *Science* 1998, *281* (5383), 1653−1656.

(34) Terenziani, F.; Morone, M.; Gmouh, S.; Blanchard-Desce, M. Linear and Two-Photon Absorption Properties of Interacting Polar Chromophores: Standard and Unconventional Effects. *ChemPhysChem* 2006, *7* (3), 685−696.

(35) Kasai, H.; Nalwa, H. S.; Oikawa, H.; Okada, S.; Matsuda, H.; Minami, N.; Kakuta, A.; Ono, K.; Mukoh, A.; Nakanishi, H. N. H. A Novel Preparation Method of Organic Microcrystals. *Jpn. J. Appl. Phys.* 1992, *31* (8A), L1132.

(36) Strickler, S. J.; Berg, R. A. Relationship between Absorption Intensity and Fluorescence Lifetime of Molecules. *J. Chem. Phys.* 1962, *37* (4), 814−822.

(37) Grabowski, Z. R.; Rotkiewicz, K.; Rettig, W. Structural Changes Accompanying Intramolecular Electron Transfer: Focus on Twisted Intramolecular Charge-Transfer States and Structures. *Chem. Rev.* 2003, *103* (10), 3899−4032.

(38) Escudero, D. Revising Intramolecular Photoinduced Electron Transfer (PET) from First-Principles. *Acc. Chem. Res.* 2016, *49* (9), 1816−1824.

(39) Terenziani, F.; Painelli, A.; Katan, C.; Charlot, M.; Blanchard-Desce, M. Charge Instability in Quadrupolar Chromophores: Symmetry Breaking and Solvatochromism. *J. Am. Chem. Soc.* 2006, *128* (49), 15742−15755.

(40) Amthor, S.; Lambert, C.; Dümmler, S.; Fischer, I.; Schelter, J. Excited Mixed-Valence States of Symmetrical Donor−Acceptor−Donor π Systems. *J. Phys. Chem. A* 2006, *110* (15), 5204−5214.

(41) Kato, S.; Matsumoto, T.; Shigeiwa, M.; Gorohmaru, H.; Maeda, S.; Ishi-i, T.; Mataka, S. Novel 2,1,3-Benzothiadiazole-Based Red-Fluorescent Dyes with Enhanced Two-Photon Absorption Cross-Sections. *Chem. - Eur. J.* 2006, *12* (8), 2303−2317.

(42) Yao, S.; Kim, B.; Yue, X.; Colon Gomez, M. Y.; Bondar, M. V.; Belfield, K. D. Synthesis of Near-Infrared Fluorescent Two-Photon-Absorbing Fluorenyl Benzothiadiazole and Benzoselenadiazole Derivatives. *ACS Omega* 2016, *1* (6), 1149−1156.

(43) Susumu, K.; Fisher, J. A. N.; Zheng, J.; Beratan, D. N.; Yodh, A. G.; Therien, M. J. Two-Photon Absorption Properties of Proquinoidal D-A-D and A-D-A Quadrupolar Chromophores. *J. Phys. Chem. A* 2011, *115* (22), 5525−5539.

(44) Sissa, C.; Terenziani, F.; Painelli, A.; Siram, R. B. K.; Patil, S. Spectroscopic Characterization and Modeling of Quadrupolar Charge-Transfer Dyes with Bulky Substituents. *J. Phys. Chem. B* 2012, *116* (16), 4959−4966.

(45) Kasha, M.; Rawls, H. R.; Ashraf El-Bayoumi, M. The Exciton Model In Molecular Spectroscopy. *Pure Appl. Chem.* 1965, *11* (3−4), 371−392.

(46) Gierschner, J.; Shi, J.; Milián-Medina, B.; Roca-Sanjuán, D.; Varghese, S.; Park, S. Luminescence in Crystalline Organic Materials: From Molecules to Molecular Solids. *Adv. Opt. Mater.* 2021, *9* (13), 2002251.

(47) Sanyal, S.; Painelli, A.; Pati, S. K.; Terenziani, F.; Sissa, C. Aggregates of Quadrupolar Dyes for Two-Photon Absorption: The Role of Intermolecular Interactions. *Phys. Chem. Chem. Phys.* 2016, *18* (40), 28198−28208.

(48) Hestand, N. J.; Zheng, C.; Penmetcha, A. R.; Cona, B.; Cody, J. A.; Spano, F. C.; Collison, C. J. Confirmation of the Origins of Panchromatic Spectra in Squaraine Thin Films Targeted for Organic Photovoltaic Devices. *J. Phys. Chem. C* 2015, *119* (33), 18964−18974.

(49) Chern, M.; Nguyen, T. T.; Mahler, A. H.; Dennis, A. M. Shell Thickness Effects on Quantum Dot Brightness and Energy Transfer. *Nanoscale* 2017, *9* (42), 16446−16458.

(50) Larson, D. R.; Zipfel, W. R.; Williams, R. M.; Clark, S. W.; Bruchez, M. P.; Wise, F. W.; Webb, W. W. Water-Soluble Quantum Dots for Multiphoton Fluorescence Imaging in Vivo. *Science* 2003, *300* (5624), 1434−1436.

(51) Wu, C.; Chiu, D. T. Highly Fluorescent Semiconducting Polymer Dots for Biology and Medicine. *Angew. Chem., Int. Ed.* 2013, *52* (11), 3086−3109.

(52) Feng, G.; Liu, B. Aggregation-Induced Emission (AIE) Dots: Emerging Theranostic Nanolights. *Acc. Chem. Res.* 2018, *51* (6), 1404−1414.

(53) Xiang, J.; Cai, X.; Lou, X.; Feng, G.; Min, X.; Luo, W.; He, B.; Goh, C. C.; Ng, L. G.; Zhou, J.; et al. Biocompatible Green and Red Fluorescent Organic Dots with Remarkably Large Two-Photon Action Cross Sections for Targeted Cellular Imaging and Real-Time Intravital Blood Vascular Visualization. *ACS Appl. Mater. Interfaces* 2015, *7*, 14965−14974.

(54) Amro, K.; Daniel, J.; Clermont, G.; Bsaibess, T.; Pucheault, M.; Genin, E.; Vaultier, M.; Blanchard-Desce, M. A New Route towards Fluorescent Organic Nanoparticles with Red-Shifted Emission and Increased Colloidal Stability. *Tetrahedron* 2014, *70* (10), 1903−1909.

(55) Daniel, J.; Bondu, F.; Adamietz, F.; Blanchard-Desce, M.; Rodriguez, V. Interfacial Organization in Dipolar Dye-Based Organic Nanoparticles Probed by Second-Harmonic Scattering. *ACS Photonics* 2015, *2* (8), 1209−1216.

(56) Luo, R.; Neu, B.; Venkatraman, S. S. Surface Functionalization of Nanoparticles to Control Cell Interactions and Drug Release. *Small* 2012, *8* (16), 2585−2594.

(57) Lescos, L.; Beaujean, P.; Tonnele, C.; Aurel, P.; Blanchard-Desce, M.; Rodriguez, V.; de Wergifosse, M.; Champagne, B.; Muccioli, L.; Castet, F. Self-Assembling, Structure and Nonlinear Optical Properties of Fluorescent Organic Nanoparticles in Water. *Phys. Chem. Chem. Phys.* 2021, *23* (41), 23643−23654.